NEW FRONT. CHEM. (**2018**)
Volume 27, Number 2, pp. 73-87
ISSN 2393-2171; ISSN-L 2393-2171

*Former: Ann. West Univ. Timisoara – Series Chem.*
*ISSN: 1224-9513*

*Review*

# ELECTROCHEMICAL SYSTEMS AND MECHANICALLY INTERLOCKED MOLECULES. PART 1: NANO-SCIENCE

**Mirela I. Iorga (1,2), Marius C. Mirica (1) and Mihai V. Putz (1,2, *)**

1. Laboratory of Renewable Energies-Photovoltaics, R&D National Institute for Electrochemistry and Condensed Matter –INCEMC–Timisoara, Timisoara, Romania
2. Laboratory of Structural and Computational Physical-Chemistry for Nanosciences and QSAR, Biology-Chemistry Department, West University of Timisoara, Timisoara, Romania

## ABSTRACT

The aim is to re-dimension More's law in nano-chemical devices by modelling quasi-particle couplings (bondonic and bondotic) as QBits impulses on chemical-physical nano-compounds (graphene lattices with Stone-Wales rotations topological defects, but also for molecules governed by nano-mechanical chemical bonds) and their propagations as dynamic donors of chemical bond and coupled electron pairs instead of electrons and single atoms as "quantum dots". This represents the quantum-chemical basis of graphenetronics (semiconductors, transistors, and integrated circuits based on topological defective graphene) and of photo-activated moletronics (molecular machines). The paper presents the correlation of quantum potentials of electrochemical tunnelling with associated electrochemical currents and with electro-photo-chemical activation mechanism of molecular machines.

**Keywords**: supramolecular systems, molecular machines, logic gates, graphenetronics, moletronics.

## 1. INTRODUCTION

In addition to macroscopic electronic devices in which information processing use electrical signals, the emphasis is now on molecular electronics, the miniaturization of electrical circuits, which can become much smaller than digital circuits manufactured on semiconductor chips [1].

These allow the investigation of the properties of molecules and supramolecular systems, such as electrical conductivity and electrical switching. Supramolecular systems may be

designed to behave like a plug/socket type macroscopic device; they are made of at least two molecular components, which must have two main properties: it must be possible to connect and disconnect the two components reversibly, and when the two elements are connected, the energy or electrons must flow from socket to plug, Figure 1.

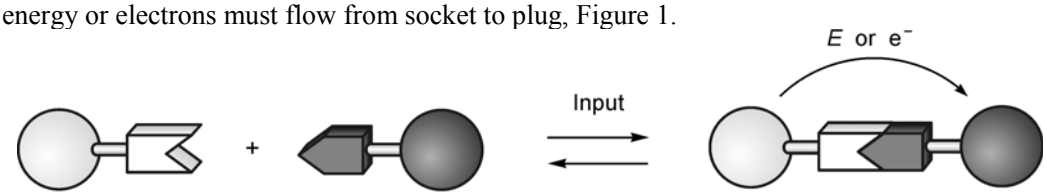


**Figure 1.** Diagram of a plug-and-socket molecular system [2]

Interactions caused by the hydrogen bonds between ammonium ions and crown ethers have been used profitably, which can be very quickly and reversibly switched on/off by acid-base inputs [2] to develop such types of devices.

***Quantum potential barriers***

The quantum model of quantum tunnelling electrons in open, dynamic systems is shown in Figure 2.

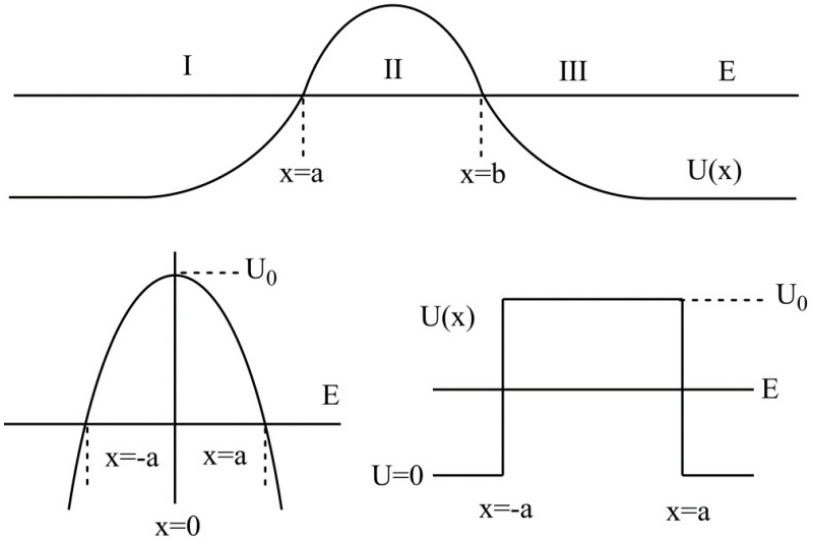


**Figure 2.** TOP: Lightly rounded potential barrier; BOTTOM-Left: Parabolic Potential Barrier; BOTTOM-right. Rectangular potential barrier (after Bockris & Khan, 1979) [3]

The expression of the total wave function of the global-local information of the system is:

- for the section I, where $U(x) \cong 0$ ; $U(x) < E$ :

$$\psi_I(x)=\frac{A}{[k(x)]^{\frac{1}{2}}}\exp\left[i\int_a^x k(x)dx\right]+\frac{B}{[k(x)]^{\frac{1}{2}}}\exp\left[-i\int_a^x k(x)dx\right] \quad (1)$$

- for section II where $U(x)>E$ :

$$\psi_{II}(x)=\frac{C}{[\kappa(x)]^{\frac{1}{2}}}\exp\left[+\int_a^x \kappa(x)dx\right]+\frac{D}{[\kappa(x)]^{\frac{1}{2}}}\exp\left[-\int_a^x \kappa(x)dx\right] \quad (2)$$

- for section III where $U(x)<E$ :

$$\psi_{III}(x)=\frac{F}{[k(x)]^{\frac{1}{2}}}\exp\left[i\int_b^x k(x)dx\right]+\frac{G}{[k(x)]^{\frac{1}{2}}}\exp\left[-i\int_b^x k(x)dx\right] \quad (3)$$

The correlation between coefficients is:

$$A=\frac{1}{2}\left[F\left(2\theta+\frac{1}{2\theta}\right)+iG\left(2\theta-\frac{1}{2\theta}\right)\right] \quad (4)$$

where:

$$\theta=\exp\left[\int_a^b \kappa(x)dx\right] \quad (5)$$

The transmission coefficient is defined as:

$$P_T=\frac{\upsilon_{trans}|\psi_{trans}|^2}{\upsilon_{incident}|\psi_{incident}|^2}=\frac{|F|^2}{|A|^2} \quad (6)$$

Because the transmission rate is $\upsilon_{trans}=\upsilon_{incident}$ and $|A|^2$ is replaced above, the case of WKB approximation (Wentzel-Kramers-Brillouin) will be considered, with the estimation of a large and high barrier, and finally the expression from Eq. (7) will be obtained.

$$P_T=\exp\left(-2\int_a^b\left\{\frac{8\pi^2 m}{\eta^2}[U(x)-E]\right\}^{\frac{1}{2}}dx\right) \quad (7)$$

This is the expression of the transmission coefficient using the general expression WKB from the above equation if both the barrier height and width are large. This represents the probability of tunneling, Gamow's equation.

In the case of a parabolic barrier, $U(x)=U_0-\frac{1}{2}fx^2$ and it has the graphical representation from Figure 2 (Bottom-Left). Then, we will get the expression of the tunneling probability for the parabolic barrier of the form:

$$P_T=\exp\left\{-\frac{\pi^2 l}{h}[2m(U_0-E)]^{\frac{1}{2}}\right\} \quad (8)$$

where the barrier width is $l=2a$ and $U_0$ represents the maximum of the barrier.

In the case of a rectangular barrier $U(x)=U_0$ and it has the graphical representation from Figure 2 (Bottom-Right), with the tunneling probability of the form:

$$H = \exp\left\{-\frac{4\pi l}{h}\left[2m(U_0 - E)\right]^{\frac{1}{2}}\right\} \quad (9)$$

where $l = 2a$ is the thickness or width of the barrier.

***Current in quantum electrochemistry***

Theoretical modeling of transient experiments in analytical electrochemistry can be achieved through a specific mathematical approach, known as the integral equation method [4]. Bonciocat [5,6] proposes that the equation describing the kinetics of a redox electrode reaction $O + ne^- \leftrightarrow R$ is an integral equation Volterra type (which is a particular case of the integral Fredholm equation), namely:

$$\boxed{i(t) = \lambda \int_0^t K(t,u) i(u) du + f(t)} \quad (10)$$

where: λ = -1; i(u), i(t): densities of the Faraday currents at time moments u < t, respectively t; K (t, u): the kernel of the integral equation and f(x) have explicit expressions containing the kinetic parameters of the electrode reaction, the concentrations, the diffusion coefficients of the electrochemically active species, the time t, u, the overvoltage at time t (Figure 3).

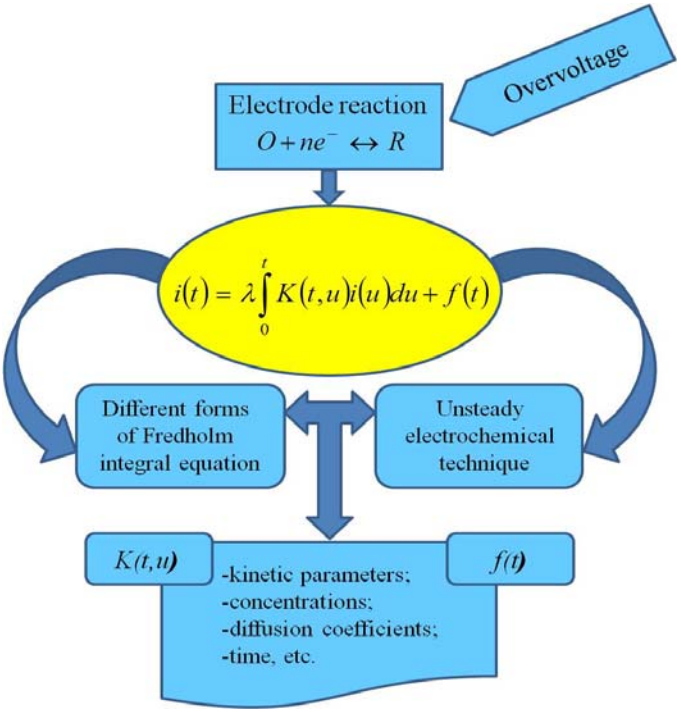


**Figure 3.** The Fredholm integral algorithm in quantum electrochemistry

By providing the only limitation by charge and mass transfer (by non-stationary diffusion) of these species, the overvoltage η(t) applied to the interface is a continuous function on the closed interval [0, a] and both functions $K\cdot(t)$ and f(t) are continuously uniform functions for t∈[0, a].

## 2. METHOD(S)/MODEL(S)

The original contribution of this paper concerns the development of the following topics:

- Nano-chemistry and multidisciplinary nano-physics;
- Graphene – from the perspective of graphite structured as multi-layer graphene;
- Quantum heterojunctions with graphene;
- Contributions to double-layer quantum electrochemistry;
- Molecular machines in the quantum-electrochemical coupling;
- Prediction of activation energies (possibly of associated micro-currents) with graphenetronic and moletronic integrated nano-systems.

The specific objectives and the results that will contribute to the achievement of these objectives are as follows: the characterization of "quantum bridges" in electrochemical systems as potentials of tunnelling and photo-electronic activation, the identification of Fredholm integral solutions for electrochemically activated currents, and the selection of quantum-molecular mechanism specific to photo-activation energies in quantum-electrochemical systems with molecular machines.

### 2.1. Theoretical Method/Model

***Potentiostatic Method***

In the case of inert metal/redox electrolyte electrodes, by following the application of a constant overvoltage, the electrode response is recorded, which in case of low overvoltages coincides with the density of the faradic current, and the Fredholm equation above becomes:

$$i(t)=\lambda\frac{i^0N}{\pi^{1/2}}\int_0^t\frac{i(u)}{(t-u)^{1/2}}du-\frac{F}{RT}i^0\eta \tag{11}$$

Finally, the equation of the potentiostatic method of low overvoltages and times is obtained:

$$i(t)=-\frac{F}{RT}i^0\eta\left(1-\frac{2i^0N}{\pi^{1/2}}t^{1/2}\right) \tag{12}$$

The obtained equations facilitate the determination of the exchange current density $i^0$ and the kinetic parameters $i^{00}$ and β of the charge transfer reaction, $\ln i^0=\ln i^{00}c_R^{\beta}+(1-\beta)\ln c_0$. In the case of an electrode made by inert semiconductor / redox electrolyte, $i_F(t)$ is the density of

the total faradic current, consisting of the contributions of the two energy bands (conduction and valence), according to the equation: $i_F(t) = i_{nF}(t) + i_{pF}(t)$;

If the charge transfer is done only through the conduction band, namely $i_p=0$, the latest equations become:

$$i(t) = -\frac{F}{RT} i_n^0 \eta \left(1 - \frac{2 i_n^0 N}{\pi^{1/2}} t^{1/2}\right), \quad \ln i_n^0 = \ln i_n^{00} c_R^{\alpha_n} + (1-\alpha_n) \ln c_0 \tag{13}$$

If the charge transfer takes place through both energy bands, the current becomes:

$$i(t) = -\frac{F}{RT} \left(i_n^0 + i_p^0\right) P \left(1 - \frac{2\left(i_n^0 + i_p^0\right) N}{\pi^{1/2}} t^{1/2}\right) \tag{14}$$

By Eqs. (13) and (14), the sum of the standard densities of the exchange currents through the two energy bands can be obtained.

***Galvanostatic method***

In case of inert metal/redox electrolyte electrodes, at low overvoltages, the current density in the outer circuit is maintained constant. The sum of the faradic and capacitive components remains constant, although their value changes over time. In this case, the Fredholm equation becomes:

$$i - i_C(t) = \lambda \frac{i^0 N}{\pi^{1/2}} \int_0^t \frac{du}{(t-u)^{1/2}} - \frac{F}{RT} i^0 \eta \tag{15}$$

The equation of the galvanostatic method for low overvoltages is obtained in two cases:

- if the capacitive current is neglected:

$$\eta(t) = -\frac{RT}{F i^0} i \left(1 + \frac{2 i^0 N}{\pi^{1/2}} t^{1/2}\right) \tag{16}$$

- if the capacitive current is taken into account:

$$\eta(t) = -\frac{RT}{F i^0} i \left(1 + \frac{2 i^0 N}{\pi^{1/2}} t^{1/2} - \frac{RT}{F} N^2 C_d i^0\right) \tag{17}$$

The obtained equations facilitate the determination of kinetic parameters $i^{00}$ and β of the charge transfer reaction.

***Linear Potential Voltammetry***

In the case of inert metal/redox electrolyte electrodes, at low overvoltages, the overvoltage applied to the electrode depends on the time and the scanning rate, according to the equation:

$$\eta(t) = v t \tag{18}$$

In this case, if the capacitive current is neglected, the Fredholm equation becomes:

$$i = \lambda \frac{i^0 N}{\pi^{1/2}} \int_0^t \frac{i(u)}{(t-u)^{1/2}} du - \frac{Fi^0}{RT} vt \tag{19}$$

and if the capacitive current cannot be ignored, the Fredholm equation will be:

$$i = \lambda \frac{i^0 N}{\pi^{1/2}} \int_0^t \frac{i(u)}{(t-u)^{1/2}} du - vC_d - \frac{2i^0 N}{\pi^{1/2}} vC_d \sqrt{t} - \frac{Fi^0}{RT} vt \tag{20}$$

Finally, the equation of linear voltammetry of potential for low overvoltages and times is obtained, in the two cases:

- if the capacitive current is neglected:

$$i(t) = -\frac{Fi^0}{RT} vt \left( 1 - \frac{4i^0 N}{3\pi^{1/2}} t^{1/2} \right) \tag{21}$$

- if the capacitive current is taken into account:

$$i(t) = -\frac{Fi^0}{RT} vt \left( 1 - \frac{4i^0 N}{3\pi^{1/2}} t^{1/2} \right) - vC_d \tag{22}$$

The obtained equations facilitate the determination of the standard density of the exchange current and the specific capacitance of the electrochemical double layer.

***Basic Faraday Impedance Method***

In the case of inert metal/redox electrolyte electrodes, a very low overvoltage is applied to the steady-state interface, analyzing the current density passing through the faradic impedance ($Z_F$) of the interface. Depending on the nature of the electrode redox reaction, a phase difference occurs between the overvoltage and the current density.

If this is irreversible, the limitations are by charge transfer, $Z_F$ is given only by the charge transfer resistance ($R_{ts}$), and the two parameters are in phase ($\varphi = 0$).

If the reaction is reversible, the limitations are by mass transfer, namely diffusion, Warburg impedance, $Z_W$, is given by the two components $R_W$ and $C_W$, and the two parameters are phase shifted with $\varphi$.

In the case of quasi-reversible reactions, all three elements ($R_{ts}$, $R_W$, $C_W$) occur, and the phase shift value $\varphi$ is based on their relative contribution. In this case, the Fredholm equation becomes:

$$i_F = I_F \sin \omega t = \lambda \frac{i^0 N}{\pi^{1/2}} \int_0^t \frac{I_F \sin \omega (t-u)}{u^{1/2}} du - \frac{Fi^0}{RT} \eta(t) \tag{23}$$

The basic Faraday impedance method determines the dependence of $R_s$ and $C_W$ on the frequency/pulse of the alternating current.

## 2.2. Experimental Method/Model

***Molecular machines with electro-photo-chemical activation***

In the case of pseudorotaxane, as shown in Figure 4 (top), their formation is favored by non-covalent interactions between the ring and the axis, which can be modulated by an external stimulus, thus controlling threading and dethreading [7-9] of molecular components. In the case of rotaxanes, two main movements with high amplitude can be made: translation by ring movement along the axis (Figure 4 – middle); rotation – by the ring movement around the axis (Figure 4 – bottom). Consequently, rotaxanes are prototypes suitable for the construction of both linear and rotary molecular machines. Indeed, systems of the first type, called molecular shuttles [10], are the most common implementation of the rotaxanes in the concept of molecular machines.

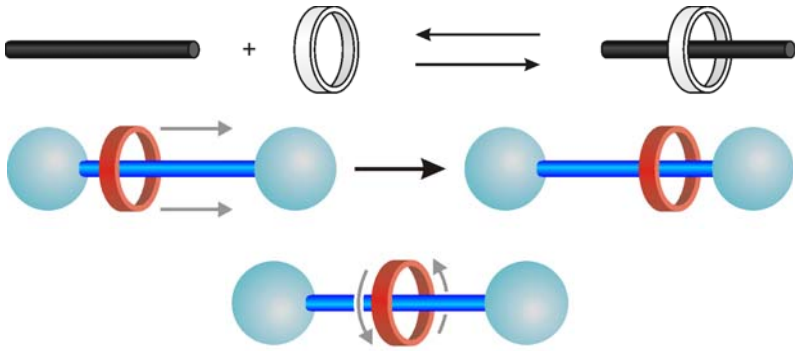

**Figure 4.** TOP: Schematic representation of the threading-dethreading equilibrium in the case of pseudo-rotaxanes, involving the axle and ring components [7-9]; MIDDLE: Schematic representation of the translational movement of the ring in the case of rotaxanes; BOTTOM: Schematic representation of the rotation of the ring in rotaxanes [10]

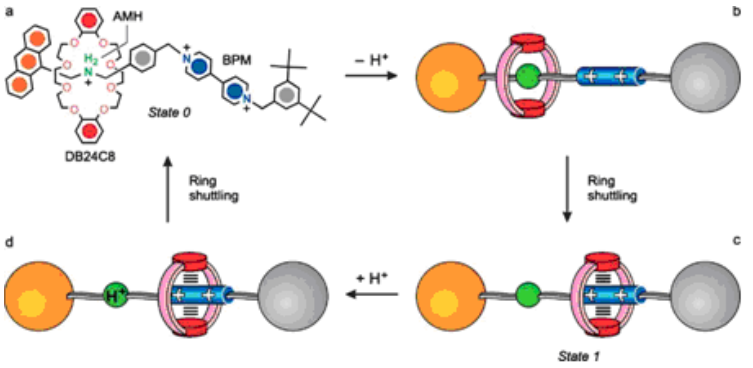


**Figure 5.** Chemical structure and operation of an acid-base controllable rotaxane (Ashton et al. 1998) [11]

An example of molecular machines that behaves as a reversible molecular shuttle is controlled by acid-base stimulation (Figure 5) [11]. It is made up of an axial component containing an ammonium ion (AMH) and an electron acceptor bipyridine unit which can

establish hydrogen bonds and charge transfer interactions with the ring component that is a dibenzo [24-]-8 crown ether. An anthracene group is used as a stopper because its absorption, luminescence and its redox properties are useful to monitor the status of the system.

As long as the interactions of the hydrogen bond $N^{+}$–H···O between the macrocyclic ring and the ammonium center are much stronger than the charge transfer interactions of the ring with the bipyridine unit, rotaxane exists only as one of the two possible translational isomers (Figure 5.a, state 0). Deprotonation of the ammonium center with a base (Figure 5.b) determines the displacement of the ring in percent of 100% by Brownian motion to the bipyridine unit (Figure 5.c, state 1); reprotoning rotaxane with an acid (Figure 5.d) directs the ring back to the ammonium center.

## 3. PERSPECTIVES

### 3.1. Rotaxane with integrated and photo-activated redox mechanism. Shuttle processes for rotaxanes

As previously mentioned, the rotaxane's common implementation in case of molecular machines is the development of molecular shuttles in which translational movements of the ring occur [12,13]. This type of molecular machines must have a well-organized structure and should work as multicomponent systems with proper functional integration [14,15].

Usually, rotaxanes are made of an axle-shaped component, equipped with two distinct recognition centers – the stations, and a ring that performs the shuttle movement between the two stations. Initially, the ring is placed on the station that is a better recognition center for it; in the case of suitably designed rotaxanes, the shuttle movement to the other station may be induced by light-powered electron transfer processes [8,16,17]. In this case, the photoinduced shuttle movement may occur, which involves the following main steps:

1. *Destabilization of the stable translational isomer*: the light excitation of the photoactive unit is followed by an electron transfer from the excited state of this unit to the ring-surrounded station, with the consequence of station deactivating;
2. *Ring movement*: the ring moves from the reduced station to the other one;
3. *Electronic Reset*: the reverse transfer of the electron from the reduced "free" station takes place to the photoactive unit, which gives the power of the electron-acceptor to this station;
4. *Nuclear Reset*: The ring moves back to the preferred station with the consecutive restoring of the structure from the beginning.

The critical points of this mechanism [8,16,18] are the competition between the photoinduction process of electron transfer and the deactivation of the intrinsically excited state, and between the shift of the ring at the reduced station and the reverse electronic transfer process. However, if the system is properly designed and optimized, each absorbed photon facilitates a forward and backward movement of the ring between the two stations, making a complete mechanical circuit.

Thus, rotaxanes of this type act as a four-stroke autonomous motor [17,18], where the visible light represents the fuel and the intramolecular processes correspond to the following stages: 1) fuel injection and combustion (destabilization of the initial structure); 2) displacement of the piston (displacement of the ring); 3) Exhaust gas evacuation (electronic

reset); 4) piston displacement (nuclear reset). Note that the photoinduced shuttle process of the ring can also occur with an external electronic relay.

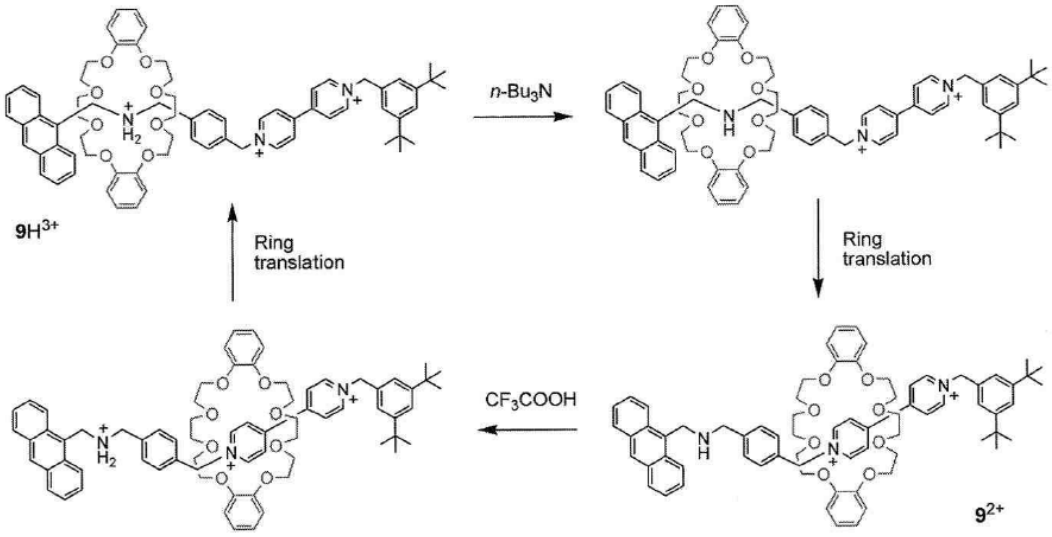


**Figure 6.** The formula of rotaxane $9H^{3+}$ structure and the representation of its functioning as a pH-controllable molecular shuttle

All the new devices and machines which can perform useful light-induced functions are of the highest importance nowadays [19].

In this context, the paper stage is in the quantum-computational modeling phase, from the perspective of the chemical reactivity, chemical electroreactivity for the complex rotaxane molecular machine presented in Figure 6. The electrochemistry of the $9H^{3+}$ [2]rotaxane is closely related to its structure, namely:

- a dibenzo[24]crown-8 ether (DB24C8) – π electron donor macrocycle;
- a dumbbell component containing a secondary ammonium center ($-NH_2^+-$) and a 4,4'-bipyridine unit ($bpy^{2+}$);
- as stoppers: a functional group of anthracene at one end, and a 3,5-di-tert-butylphenyl group at the other end,

and also, besides the in silico – in vitro complete characterization, aims its subsequent functionalization in the graphene matrix, with the perspective of replacing moletronics with molecular circuits integrated on graphene, in graphenetronic engineering of carbon microcircuits with a molecular capacitor.

## 3.2. Chemical Electro-Reactivity with Molecular Machines. From moletronics to inclusive graphenetronics

As in the case of electrons, photons play a double role [8,20], namely: they supply the energy required by the system and have the ability to highlight changes induced in the system – which means that photons can also be used to write and read the status of the system [21].

The photoinduced energy and electron transfer reactions can be exploited to connect light-supplied energy with the mechanical, electrical and optical functions of molecular devices and machines [17,21]. These processes represent the basis of the bottom-up construction of light-powered nanoscale devices and machines [22].

Thus, the general acid-base processes are transposed at the electrochemical level by photoactivation of the molecular machines, by the following process sequences occurring in a supramolecular system A-L-B type [7,22], where:

- A is the molecular unit that absorbs light;
- B is another molecular unit involved in light-supplied processes;
- L is the connection unit (also known as "bridge").

Under the influence of excitation light, the photoexcitation process takes place according to the equation:

$A–L–B + h\nu \rightarrow {}^*A–L–B$ *photoexcitation*

In this case, the two partner reactions are already of convenient duration and may undergo the transfer of electrons in the variants:

$^*A–L–B \rightarrow A^+–L–B^-$ *oxidative transfer of electrons*

$^*A–L–B \rightarrow A^-–L–B^+$ *reductive transfer of electrons*

$^*A–L–B \rightarrow A–L–{}^*B$ *electronic energy transfer*

In the absence of further processes (such as decomposition of oxidized or reduced species), photoinduced electron transfer processes are followed by spontaneous reverse electron transfer reactions that regenerate the initial state of the system:

$A^+–L–B^- \rightarrow A–L–B$ *oxidative reversed electron transfer*

$A^-–L–B^+ \rightarrow A–L–B$ *reductive reversed electron transfer*

and the photoinduced energy transfer is followed by the radiation or non-radiation deactivation of the excited acceptor:

$A–L–{}^*B \rightarrow A–L–B$ *degradation of the excited state*

In supramolecular systems, electron and energy transfer processes can often involve exciting states with very short lifetimes.

The current challenge resides in the identification of functionalized graphene devices with photo-activated molecular machines based on the sequences of the processes as mentioned above, and their proper selection, respective deca-nano-graphenic integration. It is not to be ignored the possibility of controlling photoisomerization, as another interesting light-induced process that can be exploited for the operation of molecular devices and machines [8,16,22].

## 4. Discussion and Conclusion

Generally, photo-electrochemical observables are monitored for the graphene nano-deca-semiconductor functionalized with molecular machines to control the Coulomb blockade (Figure 7), with various graphene integration phases observed by atomic force microscopy.

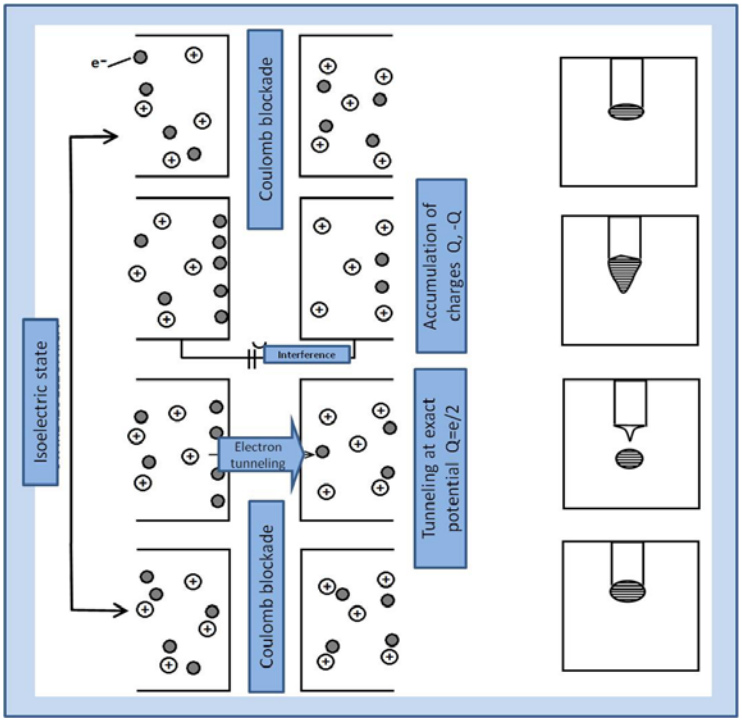


**Figure 7.** Nano-electro-scopic phenomenology of the Coulomb blockade (left), and its macroscopic correspondence (right)

In the present case, the phenomenon of the Coulomb barrier involves three correlated aspects, namely:

- the occurrence of a band gap (BI) around the Fermi level in the energy spectrum of electrons limited in semiconductor quantum dots or in small metallic particles (generically speaking, in islands) that are coupled to metallic wires by tunneling barriers;
- BI – the additional energy required due to the Coulomb interaction between the electrons of the island, for an electron to tunnel into or from the island;
- tunneling/redistribution of electrical charge – expressed by a change in the electrostatic potential.

Once optimized, the Coulomb blockade allows precise control of a small number of electrons with essential applications in switching devices with low power dissipation and thus an increase in the circuit integration level.

For the next step – the functionalization of graphene matrices with molecular machines, the successive actions are:

- the structures of molecular machines (rotaxanes/catenanes) considered more important are represented in Hyperchem [23];
- the chemical reactivity, transfer energy and other parameters that can be obtained based on the HSAB are calculated;
- for the studied systems, the Coulomb blockade is estimated;
- predictions are made on the photovoltaic effect bondonic type, using bondonic spectral relations;

- the thermodynamic indices of interconversion (free energy, enthalpy, entropy, etc.) in the case of molecular machines, are calculated through the path integral formalism;
- by the similarity between molecular machines and binary logic systems (Figure 8) the logical amount of information is provided, estimating the type of logic system (AND, OR, XOR, etc.) corresponding to the state of the molecular machine during operation.

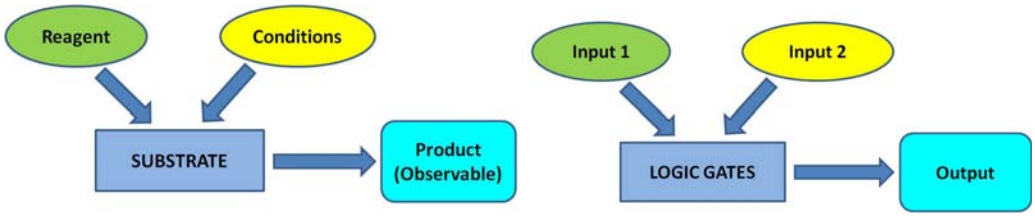


**Figure 8**. The schematic representation of the similarity between a chemical process (left) and a logical system (right)

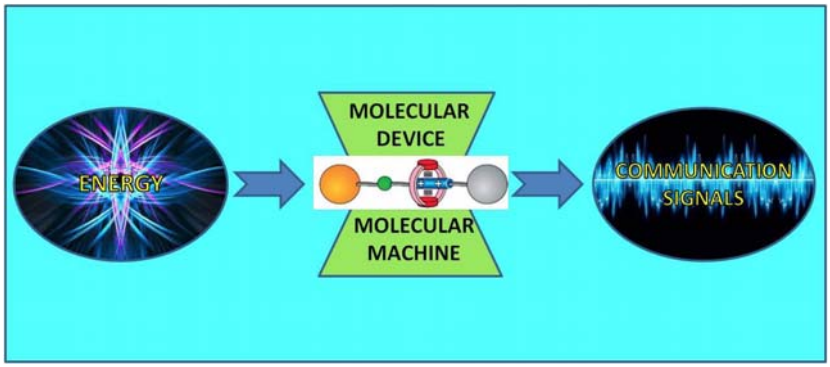


**Figure 9.** Sustainable transfer from energy to information with the aim of molecular machines integrated into devices, molecular and graphenetronic

Finally, the molecular machines – by functionalizing the quantum deca-nano-quantum semiconductor, which is integrated as an electronically activated microcircuit, provide electro-logical, controlled, activated, intelligent and sustainable functions (Figure 9), as follows:

- represents switches at which the output (0 or 1) depends on the input (0 or 1);
- can generate the AND logic gate – the logic product between the inputs, the output signal is 1, all the inputs are 1; the equivalent circuit consists of switches in series;
- can generate OR logic gate – the logic sum between inputs, the output signal is 1, if at least 1 of the inputs has the value 1; the equivalent circuit consists of switches in parallel;
- can generate the XOR (eXclusive OR) logic gate – more complicated than the AND and OR logic gates, and the logic circuit contains two bipolar switches; output – as in the case of OR logic gate but is 0 if both inputs are 1; basically, this is a comparator that can determine whether two inputs have the same value;
- ensures the development of molecular systems that act as logic circuits;
- represent systems that convert the input stimulus (optical, electrical or chemical) = input into output signals (which may also be of optical, electrical or chemical nature) = output.

## ACKNOWLEDGEMENT

We hereby acknowledge the research project PED123/2017 of UEFISCDI-Romania.

## REFERENCES

1. Reed, M.A. Molecular-scale electronics, *Proceedings of the IEEE* **1999**, *87*, 652-658.
2. Venturi, M.; Balzani, V.; Ballardini, R.; Credi, A.; Gandolfi, M.T. Towards molecular photochemionics, *Int. J. Photoenergy* **2004**, *6*, 1-10.
3. Bockris J.O'M., Khan, S.U.M. *Quantum Electrochemistry*, Plenum Press, New York, USA, **1979**.
4. Bieniasz, L.K. *Modelling Electroanalytical Experiments by the Integral Equation Method*, Springer Verlag Berlin, **2015**.
5. Bonciocat, N. *Electrochimie și aplicații*, Ed. Dacia Europa-Nova, Timișoara, România, **1996**.
6. Bonciocat, N. *Alternativa Fredholm în Electrochimie*, Ed. Mediamira, Cluj-Napoca, România, **2005**.
7. Balzani, V.; Credi, A.; Venturi, M. *Molecular Devices and Machines. Concepts and Perspectives for the Nanoworld*, Wiley-VCH, Weinheim, **2008a.**
8. Balzani, V.; Credi, A.; Venturi, M. Light powered molecular machines, *Chem. Soc. Rev.* **2009**, *38*, 1542-1550.
9. Ragazzon, G.; Baroncini, M.; Silvi, S.; Venturi, M.; Credi, A. Light-powered, artificial molecular pumps: a minimalistic approach, *Beilstein J. Nanotechnol.* **2015a,** *6,* 2096-2104.
10. Balzani, V.; Bergamini, G.; Ceroni, P.; Vogtle, F. Electronic spectroscopy of metal complexes with dendritic ligands, *Coord. Chem. Rev.* **2007**, *251*, 525-535.
11. Ashton, P.R.; Ballardini, R.; Balzani, V.; Baxter, I.; Credi, A.; Fyfe, M.C.T.; Gandolfi, M.T.; Gómez-López, M.; Martínez-Díaz, M.-V.; Piersanti, A.; Spencer, N.; Stoddart, J.F.; Venturi, M.; White, A.J.P.; Williams, D.J. Acid-base controllable molecular shuttles, *J. Am. Chem. Soc.* **1998**, *120*, 11932-11942.
12. Bissell, A.; Cordova, E.; Kaifer, A.E.; Stoddart, J.F. A chemically and electrochemically switchable molecular shuttle, *Nature* **1994**, *369*, 133-137.
13. Arduini, A.; Bussolati, R.; Credi, A.; Pochini, A.; Secchi, A.; Silvi, S.; Venturi, M. Rotaxanes with a calix[6]arene wheel and axles of different length. Synthesis, characterization, and photophysical and electrochemical properties, *Tetrahedron* **2008**, *64*, 8279-8286.
14. Balzani, V.; Credi, A.; Venturi, M. Molecular machines working on surfaces and at interfaces, *Chem. Soc. Rev.* **2008b**, *9*, 202-220.
15. Balzani, V.; Bergamini, G.; Ceroni, P. From the photochemistry of coordination compounds to light-powered nanoscale devices and machines, *Coord. Chem. Rev.* **2008c**, *252,* 2456-2469.
16. Credi, A.; Venturi, M. Molecular machines operated by light, *Cent. Eur. J. Chem.* **2008**, 6, 325-339.
17. Balzani, V.; Bergamini, G.; Marchioni, F.; Ceroni, P. Ru(II)-bipyridine complexes in supramolecular systems, devices and machines, *Coord. Chem. Rev.* **2006a**, *250,* 1254-1266.

18. Balzani, V.; Credi, A.; Venturi, M. Controlled disassembling of self-assembling systems: Toward artificial molecular-level devices and machines, *Proc. Natl. Acad. Sci. USA* **2006b**, *99*, 4814-4817.
19. Venturi, M.; Iorga, M.I.; Putz, M.V., Molecular Devices and Machines: Hybrid Organic-Inorganic Structures, *Current Organic Chemistry* **2017**, *21*, 27, p.2731-2759.
20. Balzani, V.; Bergamini, G.; Ceroni, P. Light: a very peculiar reactant and product, *Angew. Chem. Int. Ed.* **2015**, *54*, 11320-11337.
21. Ceroni, P.; Credi, A.; Venturi, M. Light to investigate (read) and operate (write) molecular devices and machines, *Chem. Soc. Rev.* **2014**, *43*, 4068-4083.
22. Balzani, V., Ceroni, P., Juris, A. *Photochemistry and Photophysics. Concepts, Research, Applications*, Wiley-VCH, Weinheim, **2014**.
23. Iorga, M.I.; Putz, M.V., Application of Molecular Machines in Photoelectrochemistry, In *Proceedings of The 24th International Symposium on Analytical and Environmental Problems*, University of Szeged, Hungary, 8-9 October 2018, Alapi T., Ilisz I., Eds., Published by University of Szeged, **2018**, pp.363-367.